NeuroImage 54 (2011) 2612–2622

Contents lists available at ScienceDirect

NeuroImage

journal homepage: www.elsevier.com/locate/ynimg

Evidence for a motor and a non-motor domain in the human dentate nucleus — An fMRI study

M. Küper [a,b,*], A. Dimitrova [a], M. Thürling [a,b], S. Maderwald [b], J. Roths [c], H.G. Elles [a], E.R. Gizewski [d,e], M.E. Ladd [b], J. Diedrichsen [f], D. Timmann [a]

[a] Department of Neurology, University of Duisburg-Essen, Germany
[b] Erwin L. Hahn Institute for Magnetic Resonance Imaging, University of Duisburg-Essen, Germany
[c] Department of Micro- and Nanotechnology, University for Applied Sciences Munich, Germany
[d] Department of Diagnostic and Interventional Radiology and Neuroradiology, University of Duisburg-Essen, Germany
[e] Department of Neuroradiology, Center for Radiology, University Hospital of Giessen and Marburg, Justus-Liebig-University Giessen, Germany
[f] Institute of Cognitive Neuroscience, University College London, UK

ARTICLE INFO

Article history:
Received 30 June 2010
Revised 21 October 2010
Accepted 8 November 2010
Available online 24 November 2010

Keywords:
Cerebellum
Cognition
Motor
Language
Visuospatial

ABSTRACT

Dum and Strick (J. Neurophysiol. 2003; 89, 634–639) proposed a division of the cerebellar dentate nucleus into a "motor" and "non-motor" area based on anatomical data in the monkey. We asked the question whether motor and non-motor domains of the dentate can be found in humans using functional magnetic resonance imaging (fMRI). Therefore dentate activation was compared in motor and cognitive tasks. Young, healthy participants were tested in a 1.5 T MRI scanner. Data from 13 participants were included in the final analysis. A block design was used for the experimental conditions. Finger tapping of different complexities served as motor tasks, while cognitive testing included a verbal working memory and a visuospatial task. To further confirm motor-related dentate activation, a simple finger movement task was tested in a supplementary experiment using ultra-highfield (7 T) fMRI in 23 participants. For image processing, a recently developed region of interest (ROI) driven normalization method of the deep cerebellar nuclei was used.

Dorso-rostral dentate nucleus activation was associated with motor function, whereas cognitive tasks led to prominent activation of the caudal nucleus. The visuospatial task evoked activity bilaterally in the caudal dentate nucleus, whereas verbal working memory led to activation predominantly in the right caudal dentate. These findings are consistent with Dum and Strick's anatomical findings in the monkey.

© 2010 Elsevier Inc. All rights reserved.

Introduction

Functional brain imaging and human cerebellar lesion studies have convincingly shown that the cerebellum contributes to cognitive function, including executive, language, and visuospatial abilities (Malm et al., 1998; Silveri et al., 1998; Fink et al., 2000, 2001; Miall et al., 2001; Gurd et al., 2002; Schmahmann, 2004; Lee et al., 2005; Ravizza et al., 2006; Frings et al., 2006; Molinari and Leggio, 2007). There is increasing evidence of a topographic organization within the human cerebellar cortex for motor and non-motor function. Recent meta-analyses of both neuroimaging and human cerebellar lesion studies suggest that sensorimotor function relies primarily on lobules I–V of the anterior lobe, adjacent parts of lobule VI, and lobule VIII of the posterior lobe, whereas cognitive functions are supported predominantly by lobules VI and VII (Stoodley and Schmahmann, 2009, 2010). In contrast, in the human very little is known about topographic organization within the cerebellar nuclei, the main output targets of the cerebellar cortex.

Anatomical studies in monkeys have shown a somatotopic organization within the dentate nucleus (Stanton, 1980; Thach et al., 1993). In contrast to the two body representations in the cerebellar cortex, only one body representation has been found in the dentate nucleus, raising the hypothesis that both body areas may converge on similar regions in the nucleus. These early findings have been extended by more recent work by Dum and Strick (2003). Using retrograde transneuronal transport of neurotropic viruses (for a review, see Strick et al., 2009), the authors found that areas located in the dorsal dentate project to the primary motor and premotor area (PMv), while more caudal and ventral areas are connected to prefrontal (Brodmann area (BA) 46, 9 L) and parietal areas (BA 7b) (Fig. 1A). Because the prefrontal and parietal areas are known to be involved in cognitive functions, Dum and Strick postulated that the dentate nucleus can be functionally subdivided into a more dorso-rostral motor domain and a more ventral and caudal non-motor domain with distinct output channels and differing antigenic properties (Pimenta et al., 2001). The dorso-caudal dentate, however,

* Corresponding author. Department of Neurology, University of Duisburg-Essen, Hufelandstrasse 55, 45122 Essen, Germany. Fax: +49 2017235721.
E-mail address: Michael.Kueper@uni-due.de (M. Küper).

1053-8119/$ – see front matter © 2010 Elsevier Inc. All rights reserved.
doi:10.1016/j.neuroimage.2010.11.028

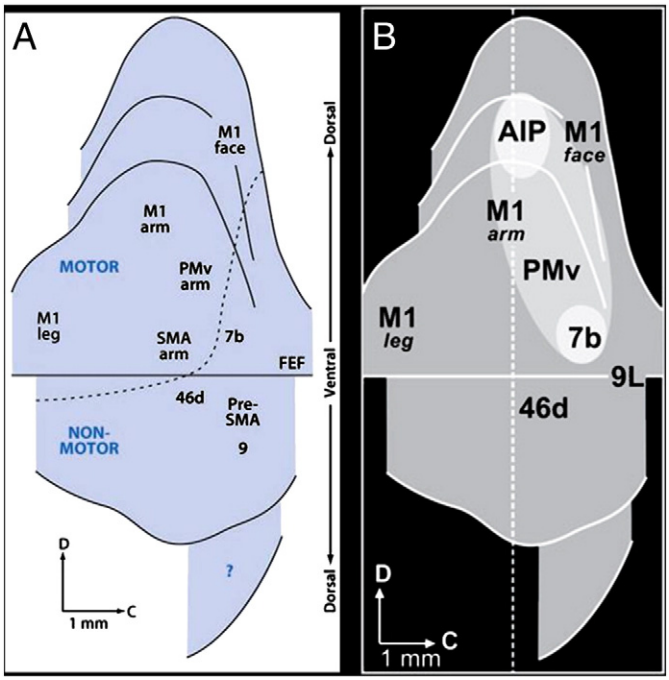

Fig. 1. Efferent cortical connections of the dentate nucleus in the macaque viewed on an unfolded map (A) published by Strick et al. (2009), used with permission. Additional projections to the AIP (B) are shown on the unfolded map published by Clower et al. (2005), used with permission. D = dorsal, C = caudal.

has also been shown to project to the anterior intraparietal area (Fig. 1B; Clower et al., 2005).

A number of functional magnetic resonance imaging (fMRI) studies in healthy human participants report activation in the dentate nucleus for both cognitive and motor tasks (Kim et al., 1994; Jueptner et al., 1997; Dimitrova et al. 2006a; Habas, 2010). Likewise, more recent resting state fMRI studies suggest that the dentate nucleus contributes to both motor and non-motor control networks (Allen et al., 2005; Habas et al., 2009). However, with one exception (Dimitrova et al., 2006a), none of these studies has made an attempt to investigate the topographic organization within the dentate nucleus.

Methodological problems are a likely reason. Blood oxygenation level dependent (BOLD) signal detection within the human cerebellar nuclei poses a difficult challenge. Due to spatial variability and the small size of the dentate, the nuclei of individual subjects reach only a maximal overlap of 70% in a standard group analysis with the widely used Montreal Neurologic Institute (MNI) 152 template (Dimitrova et al., 2006b). Thus, the chance that functionally corresponding subregions of the cerebellar nuclei superimpose across participants with common normalization methods is quite small. Worse still, there is a substantial danger that reported activations of the deep cerebellar nuclei (DCN) are due to physiological artifacts or smoothed activation from the surrounding gray matter. In the present study, we therefore employed a recently developed new normalization approach (Diedrichsen et al., 2010). We utilized the fact that the dentate nucleus, due to its high iron content, can be clearly seen on T2-weighted scans as a hypointensity. We used this information to ensure overlap of the deep cerebellar nuclei after normalization.

We asked the question whether a division into motor and non-motor areas as proposed by Dum and Strick (2003) can be found in the human dentate using 1.5 T fMRI. To address this question, we compared activation in finger tapping motor tasks of different complexities and two cognitive tasks. We expected that finger movements would activate predominantly the more rostral parts of the ipsilateral dorsal dentate, whereas the cognitive tasks would activate the caudal parts of the dentate. The cognitive conditions comprised a verbal working memory and a visuospatial task. Based on the connections of the cerebellar hemispheres with the contralateral cerebrum, the right cerebellar hemisphere is thought to support language function, and the left hemisphere visuospatial function (Fink et al., 2000; Stoodley and Schmahmann, 2009). Therefore, activity related to verbal working memory was expected primarily in the right dentate and activity related to the visuospatial task primarily in the left dentate. To further substantiate the findings of a motor area within the dentate nucleus a supplementary experiment was performed using ultrahigh-field MRI (7 T). The increased signal-to-noise ratio in the 7 T MRI field was considered helpful confirming the existence of a motor area within the dorso-rostral dentate.

Experiment 1 (1.5 T MRI data set)

Methods

Participants

A total of 19 healthy participants (7 male/12 female, mean age of 27.8 ± 6.3 years) were included. Six participants were excluded from the analysis, three due to insufficient task performance, three because no reliable BOLD signal could be measured in the dentate (see below). Data of thirteen participants (5 male/8 female, mean age 30.1 ± 7.2 years) were included in group statistical analysis. All participants were right-handed as measured by the Edinburgh handedness scale (Oldfield, 1971). Neurological examination performed by one of the authors (MK) was unremarkable in all participants. None of the participants took centrally acting medication at the time of the testing. Informed consent was obtained from all the participants. The study was approved by the local ethics committee.

fMRI data acquisition

A Siemens 1.5 T Sonata system (Siemens, Erlangen, Germany) was used to acquire BOLD contrast-weighted echoplanar images (EPIs) for functional scans. Thin slices were acquired of the cerebellar region containing the nuclei using high spatial resolution. All fMRI images were acquired with an eight-channel head coil using standard imaging (Gizewski et al., 2005). For each subject the roof of the fourth ventricle was identified on the localizer scan, and 10 continuous, 2.5 mm thick axial slices parallel to AC–PC line were acquired covering the region posterior to the roof of the fourth ventricle as described previously (Dimitrova et al., 2006a). Each EPI session consisted of 135 mosaic scans with matrix size = 128 × 128 × 10, TR = 3000 ms, TE = 55 ms, FOV = 230 mm, flip angle = 90° and voxel size = 1.8 × 1.8 × 2.5 mm^3. Because of magnetization relaxation effects, the first five volumes in each session were discarded from further analysis. A three-dimensional (3D) sagittal volume of the entire brain was acquired using a T1-weighted magnetization prepared rapid acquisition gradient echo sequence (MPRAGE; TR = 2400 ms, TE = 4.38 ms, FOV = 256 mm, 160 slices, voxel size 1 × 1 × 1 mm^3).

Experimental conditions

A block design was used with seven 30 s rest and six 30 s active blocks (a total of 135 scans). The participants had to perform four experimental tasks including two motor and two cognitive (verbal working memory and visuospatial navigation) tasks with two control conditions. Each task and control condition was performed in a separate fMRI run. Prior to imaging participants were briefly trained outside the scanner on how to perform each of the tasks. In addition, a 30 s training block was done in the scanner before each of the six fMRI runs was started. The sequence of the tasks and control conditions was randomized between participants. Visual stimuli were generated by a PC system running E-PRIME software (http://www.pstnet.com/eprime.cfm) and presented via a projector onto a screen. Visual

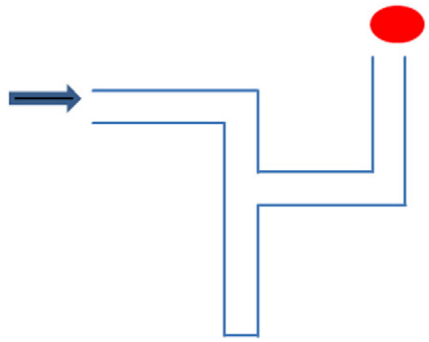

Fig. 2. Example of a labyrinth in the visuospatial task. Participants had to navigate through the labyrinth with four joystick movements, starting at the black arrow and ending at the red circle. For this labyrinth movements had to be right-down–right-up.

images were viewed from a mirror mounted on the eight-channel head coil. Eye movements were not recorded.

Simple motor task. An optical response keypad (LUMItouch, Photon Control Inc., USA) was positioned on the participants' right thigh. The keypad had four buttons, arranged in a horizontal row, with an inter-button distance of 1.5 cm. Participants used their right index finger to press the button at the right end repeatedly. Finger tapping had to be synchronized (one tap per click) to auditory clicks (50 ms duration, 750 Hz), which were presented via headphones with a frequency of 3 Hz. Participants were asked to keep their eyes closed.

Complex motor task. The same optical response keypad was used as described above. Participants used their right index finger to press the four buttons in the following sequence: 1–2–3–4–4–3–2–1. Again, finger tapping had to be synchronized to auditory clicks and participants were asked to keep their eyes closed.

Visuospatial navigation task. In this condition participants navigated through a labyrinth (starting at the arrow as shown in Fig. 2) with a custom-made optical response joystick. Participants used a power grip to operate the joystick. First, the labyrinth was visually presented for 2 s, then auditory clicks (1 Hz) started and participants had to navigate through the labyrinth using 4 joystick movements (e.g. right, down, right, up for the labyrinth shown in Fig. 2), synchronized to the clicks. No visual feedback of the joystick movements was provided. In each of the 30 s active blocks, 5 different labyrinths were presented and changed trial by trial.

Visuospatial navigation control condition. The control condition was the same as the visuospatial navigation task, except that within each of the 30 s active blocks always the same labyrinth was presented and had to be navigated 5 times in a row. A new labyrinth was shown at the beginning of each of the six active 30 s blocks.

Verbal working memory. In this task participants had to memorize a four-digit sequence, consisting of digits from 1 to 4 (e.g. 2–3–2–4). The sequence was visually presented for 1 s (Fig. 3). Thereafter, participants had to press the same sequence within 2 s using the four buttons of the optical response keypad with their right index finger. Prior to fMRI scanning, participants were instructed that the left button corresponded to digit 1, the middle left button to 2, the middle right button to 3, and the right button to 4. As in the motor task, the taps had to be synchronized to clicks (2 Hz) presented via headphones, while a fixation cross was shown instead of the number sequence. In each 30 s block, 10 different number sequences were presented. During the 30 s rest periods the fixation cross was displayed.

Working memory control condition. The control condition was the same as the working memory task, except that the digits did not vanish after 1 s. That is, participants were not required to memorize the digits but could simply press the buttons on the response keypad according to the digit sequence seen on the screen.

Analysis of behavioural data

For the motor and working memory tasks a four button optical response keypad (LUMItouch, Photon Control Inc., USA) was used. Tapping movements were electronically recorded and monitored outside the scanner by the experimenter. Task performance was analyzed off-line using custom-made software. The number of tapping movements achieved and sequence errors were calculated.

For the visuospatial navigation task a custom-made optical response joystick was used. Joystick movement onset was recorded. The quality of the recordings, however, was not accurate enough to allow quantitative analysis. Movement directions were visually controlled by one investigator (MK) from outside the scanner.

Image analysis

The functional imaging data were analyzed using (SPM5) (Wellcome Department of Cognitive Neurology, London, UK). First, EPI images were realigned to correct for head motion, resulting in the creation of a mean EPI image. No data set exhibited head motion greater than 2 mm in translation or 2 mm in rotation. The mean image was then coregistered to the anatomical T1 image of the individual participant. The automatic co-registration was refined manually to ensure the fit of the cerebellar structures. For the statistical 1st level analyses, a general linear model was then applied (Friston et al., 1995) to the realigned, but otherwise unsmoothed, EPI images. The time series of each voxel was fitted with a corresponding task regressor that modeled a box-car convolved with a canonical hemodynamic response function. A temporal high-pass filter (cut off 128 s) was used to correct for the low-frequency drifts in the data, and serial autocorrelations were taken into account by means of an AR(1) correction. For each of the experimental tasks and control conditions, a significant change of the BOLD effect compared to the rest condition was tested by specifying the appropriate contrast.

Cerebellar cortex. For the normalization of the cerebellar cortical data, T1-weighted images were deformed to fit the spatially unbiased atlas

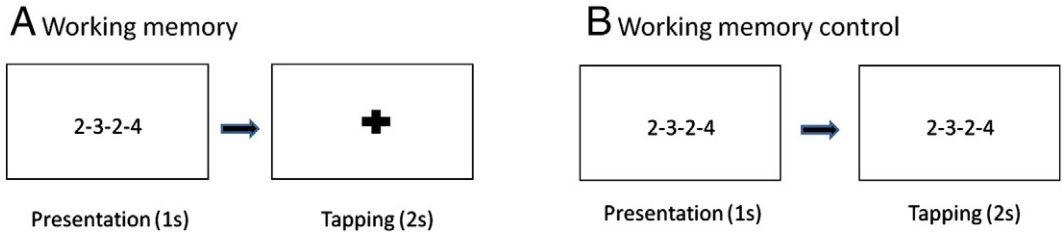

Fig. 3. Visual presentations in verbal working memory (A) and verbal working memory control condition (B). In the verbal working memory task, a four-digit sequence was displayed for 1 s, then a fixation cross appeared and participants had to tap the sequence. In the control condition, the sequence remained on the display while tapping.

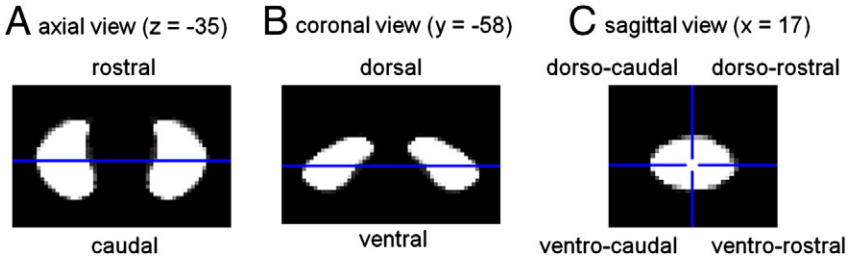

Fig. 4. Subdivision of the dentate shown on the dentate nucleus template (Diedrichsen et al., 2010). A) Blue line indicates the border between rostral and caudal domain between y coordinates −58 and −59. B) Blue line indicates the border between dorsal and ventral domain between z coordinates −35 and −36. C) Left dentate, sagittal view. Blue crosshair (x = 17, y = −58, z = −35) subdivides dentate into dorso-caudal (upper left quadrant), dorso-rostral (upper right quadrant), ventro-caudal (lower left quadrant), and ventro-rostral (lower right quadrant) subdomains.

template (SUIT) of the human cerebellum (Diedrichsen, 2006). This non-linear deformation was then applied to each contrast image from the individual participants. The normalized images were then smoothed with a Gaussian kernel of 4 mm full width at half maximum (FWHM). Image acquisition was restricted to the cerebellar region that contained the dentate and therefore excluded parts of the superior and inferior cerebellar cortex for the 1.5 T data set. Within the field of view were lobule VI, X, and Crus I, inferior parts of lobule V as well as superior parts of lobule VII, VIII, IX, and Crus II (see also Fig. 5).

Dentate nucleus. The dentate nuclei were identified as hypointensities on the mean image and marked as the region of interest (ROI) using MRICRON software (www.sph.sc.edu/comd/rorden/mricron/). In accordance with a previous study of our group (Dimitrova et al., 2006a), only participants with detectable dentate activation ($p<0.005$ uncorrected, extension threshold 0 voxel) in individual SPM contrast images in at least one of the experimental tasks without any normalization or smoothing were included in 2nd level statistical group analyses. Based on this criterion, three participants were excluded from final analysis. High iron content of the dentate causing BOLD signal loss is a likely reason for lack of activation.

For normalization, we used a modified version of the SUIT method. This normalization algorithm tries to deform the T1 image so that it fits to the SUIT template, while optimizing the overlap between the ROI and a dentate template that was developed as an average of 23 healthy control subjects participating in another study (Diedrichsen et al., 2010). This method ensures a near-perfect overlap between the nuclei of individual participants, while preserving a good normalization of other structures. To avoid smoothing of activation surrounding the dentate nucleus into the ROI, the functional images were masked with the dentate ROI before normalization. The normalized functional data from the dentate nuclei were resampled at $1\times1\times1$ mm^3 resolution and then smoothed with a 2 mm kernel. The small smoothing kernel was chosen in order to preserve functionally different dentate subdomains as far as possible. Group analysis was performed at a threshold of $p=0.005$ uncorrected (unc.). The random field (RF) cluster size correction was not considered suitable for these data sets, because the search volume was very small and because the smoothness of images was low compared to the image resolution (Hayasaka and Nichols, 2003). Bootstrap analysis was therefore used to correct the significance level for multiple tests (Hayasaka and Nichols, 2003). Sets of 13 random samples were drawn from all contrast images for the 1.5 T data set (with replacement), and each multiplied independently with 1 or −1 to randomize the sign. For each of these fake data sets, a t-map was calculated and the maximal t-value and cluster size were determined at the uncorrected threshold ($t(13)=3.05$, $p=0.005$), searching both in the left and right dentate. Repeating this process 10,000 times, the threshold values were determined that would only occur in 5% of the random data sets. The corrected peak t-value was 5.22 and the minimal cluster size 34 mm^3 (at $t=3.05$). If either criterion was fulfilled, activation was regarded as significant.

To describe the localization of dentate activations, the dentate template was divided into four sections. In accordance with Dum and Strick (2003; see Fig. 1), the dentate was subdivided into a dorso-rostral (DRDN), dorso-caudal (DCDN), ventro-rostral (VRDN), and ventro-caudal (VCDN) section. The border between the rostral and caudal dentate was set between $y=-58$ and $y=-59$, which corresponds to the middle of the maximum extension of the dentate atlas space in the rostro-caudal direction in the axial plane ($y=-48$ to -68 mm) (Fig. 4). The border between the ventral and dorsal dentate was set between $z=-35$ and $z=-36$, which corresponds to the middle of the maximum extension of the dentate atlas space in the ventro-dorsal direction ($z=-30$ to -41 mm) in the sagittal plane (Fig. 4).

For reasons given below, condition averages were also considered. An average contrast comprising all experimental tasks and control conditions was calculated. In addition, an average contrast including both cognitive tasks with subtraction of the simple motor task ("cognitive vs. simple motor") was created. To test for significant effects of lateralization, further statistical analysis of beta estimates within each dentate subdomain was performed. An additional participant-wise analysis was performed, which is provided as supplementary material.

Results

Behavioural data

The number of achieved tapping movements per block was close to the expected number of movements in the verbal working memory task and the control task (Table 1). In the motor tasks, the number of achieved movements was on average below the expected number of movements. The most likely reason was that the required tapping frequency (3 Hz) was high. Furthermore, many subjects showed a short delay of 1–2 s between the start of the clicks and the start of tapping movements.

Error rates observed in the complex motor task were significantly higher ($p=0.009$, paired t-test) than in the simple motor task. In the

Table 1
Mean number of tapping movements and error rates per 30 s block (mean ± SD) in the motor and verbal working memory tasks in the 13 participants included in the fMRI analysis. Errors were defined as tapping of incorrect sequences.

	Expected number of movements	Achieved number of movements	Error rate
Simple motor	90	84.3 ± 8.7	2.1 ± 3.4%
Complex motor	90	82.5 ± 16.7	3.9 ± 4.2%
Working memory	40	40 ± 3	16.5 ± 12%
Working memory control	40	40.3 ± 1.1	11.8 ± 12.8%

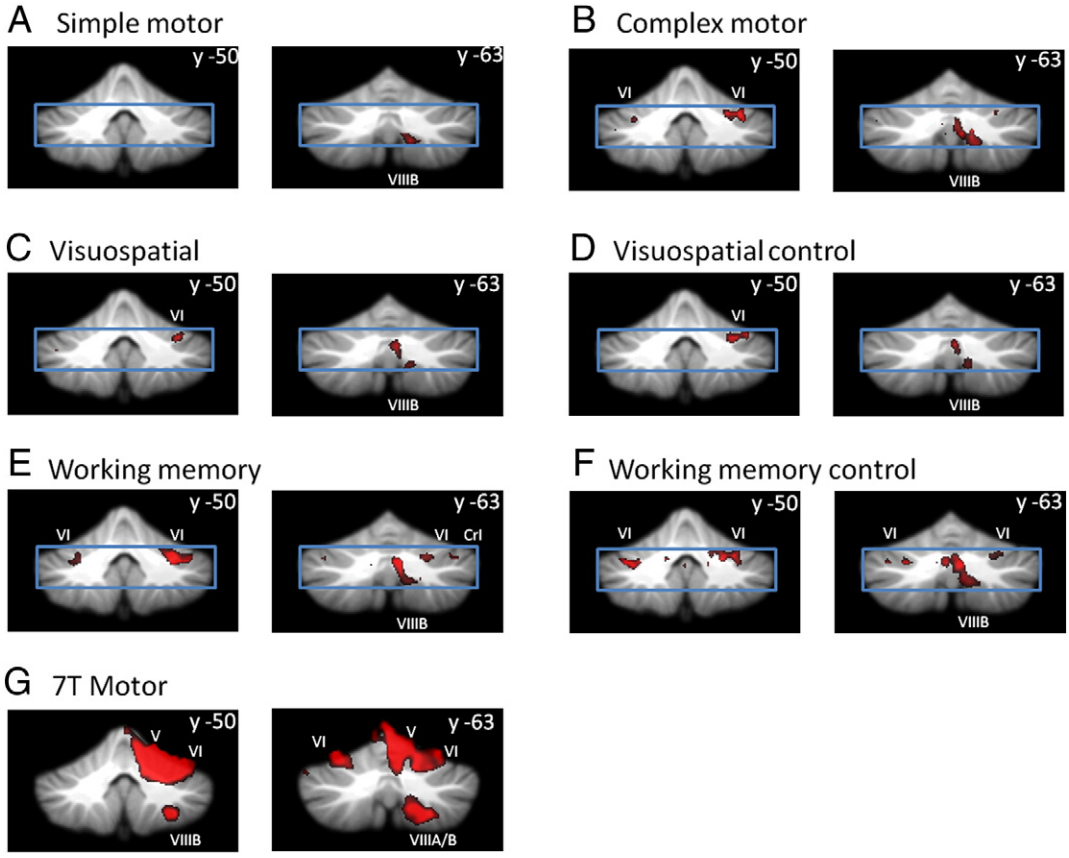

Fig. 5. Cerebellar cortical activations of the simple motor task (A), complex motor task (B), visuospatial task (C), visuospatial control condition (D), working memory task (E), working memory control condition (F), and 7 T motor task (G) mapped onto coronal sections of the SUIT template (Diedrichsen, 2006) in MRICRON (threshold t = 4, peak t = 6). Blue box indicates the field of view. Lobule identification was performed with the help of a probabilistic MR atlas of the cerebellum (Diedrichsen et al., 2009).

verbal working memory task, mean error rate did not differ significantly from the control condition ($p = 0.153$). Participants with an error rate exceeding two standard deviations from the mean of all participants were excluded. Based on this criterion, three participants were excluded from the fMRI statistical analysis, one participant because of insufficient task performance in the complex motor task (mean error rate 61.9% per 30 s block) and two participants in the verbal working memory task (mean error rate of 52% and 48% per 30 s block).

Cerebellar cortical activations

Because slice selection focused on the dentate nucleus, only the middle part of the cerebellar cortex was covered (Fig. 5). Despite this, one could see the fringes of the motor task activations of the known hand areas within the anterior and posterior cerebellum (Rijntjes et al., 1999; Grodd et al., 2001; Stoodley and Schmahmann, 2009). Bilateral activation of lobule VI was observed, predominantly on the right (that is ipsilateral to the movement) and right-sided activation of lobule VIII A (Table 2, Fig. 5). Activation in the

Table 2
Local maxima of activation within the cerebellar cortex ($p < 0.001$ unc., minimum 50 mm^3). Peak location is underlined.

Contrast	Side	x,y,z	Location	Cluster size	t-value
Simple motor	Right	6, −66, −42	VIII A, VIII B	63 mm^3	5.88
Complex motor	Right	30, −40, −36	VI, V	103 mm^3	10.8
	Right	6, −70, −36	VII B, VIII A, VIII B	247 mm^3	9.6
	Left	−34, −44, −32	VI, V, Crus I	65 mm^3	7.1
Visuospatial	Right	4, −70, −36	VIII A, VII B, Crus II, VIII B	237 mm^3	8.79
	Right	32, −40, −30	VI, V, Crus I	90 mm^3	7.1
Visuospatial control	Right	6, −68, −36	VIII A, VII B, Crus II, VIII B	105 mm^3	6.8
	Right	44, −58, −28	Crus I, VI, V	189 mm^3	6.42
Working memory	Right	6, −72, −36	VIII A, VII B, Crus II, VIII B	381 mm^3	9.37
	Right	30, −48, −32	VI, V, Crus I	404 mm^3	8.87
	Left	−28, −38, −36	VI, V, Crus I	171 mm^3	6.73
Working memory control	Right	24, −56, −28	VI, V, Crus I	382 mm^3	11.21
	Right	6, −70, −34	VIII A, VII B, Crus II, VIII B	454 mm^3	10.92
	Left	−28, −60, −32	VI, Crus I	287 mm^3	9.18
7 T motor	Right	23, −51, −18	V, IV, VI, VIII A, VIII B, Crus I Left: IV, V, VI, Crus I	34573 mm^3	11.88
	Left	−33, −56, −48	VII B	81 mm^3	4.19
	Left	−23, −64, −54	VIII A	52 mm^3	3.99

simple motor task was lower and located primarily in ipsilateral lobule VIII. Known hand areas were also activated in the working memory and visuospatial tasks and in the control conditions. In the visuospatial task and control condition, activations of the hand areas were restricted to the right side, ipsilateral to the movement. Activations of bilateral lobule VI were more extended in the verbal working memory task. Again, lobule VI was predominantly activated on the right. Activation of Crus II was exclusively found in the cognitive tasks and their control conditions, while Crus I was also activated in the complex motor task. A direct comparison of the cognitive tasks and control conditions, however, did not result in any significant activation.

Dentate nucleus activations

Dentate nucleus activations are shown superimposed on the template of the right dentate nucleus in Fig. 6 and of the left dentate nucleus in Fig. 7. Local maxima are summarized in Table 3. In both the simple and complex motor tasks, no suprathreshold cluster of activation was detected. In contrast, the more demanding cognitive tasks resulted in reliable dentate activity.

In the visuospatial navigation task, symmetric clusters within the dorso-caudal dentate nucleus were detected bilaterally (Figs. 6A, 7A). Highest t-values were observed on the left, while the cluster size was larger on the right. The cluster on the left also extended into the dorso-rostral domain. In the visuospatial control task, strong activation of the ventro-caudal dentate nucleus was found on the right side with minimal extension into the bordering dorso-caudal part (Figs. 6B, 7B). There was no activation present on the left.

In the verbal working memory tasks, significant activation was most pronounced on the right within the ventro-caudal area with little extension to the dorso-caudal part (Fig. 6C). On the left side, two less significant clusters were present (Fig. 7C). One cluster peaked ventro-caudally close to the center of the nucleus and also comprised dorso-caudal, and ventro-rostral parts. The other cluster on the left involved ventro-rostral and dorso-rostral parts. Right-sided activation was also observed in the verbal working memory control task, with activation located dorso-caudally and extending to the ventro-caudal part (Fig. 6D). On the left, two clusters were found with activation of ventro-rostral, ventro-caudal, and dorso-caudal parts similar to the verbal working memory task (Fig. 7D).

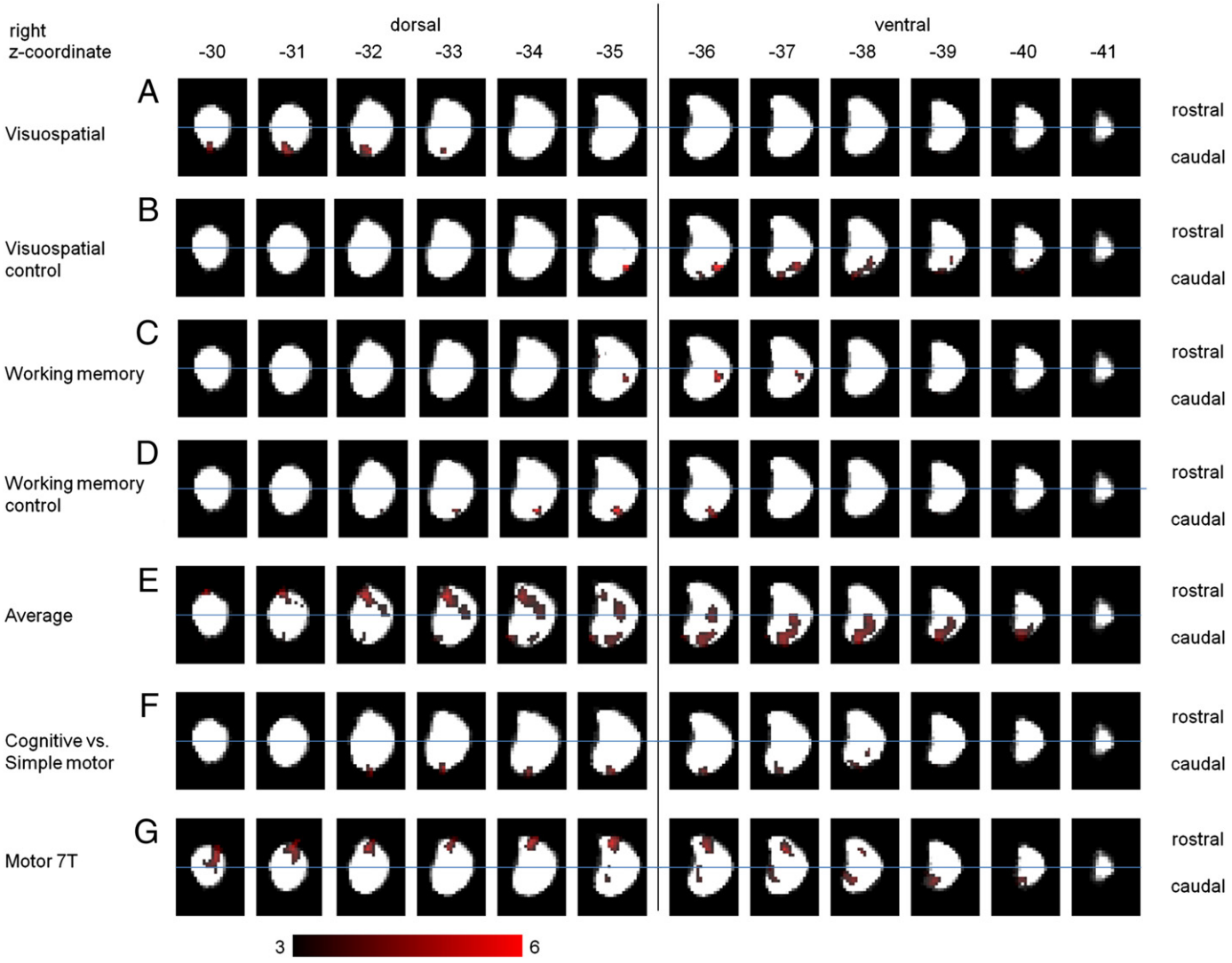

Fig. 6. Significant dentate nucleus activations superimposed on the template of the right nucleus in axial orientation (Diedrichsen et al., 2010) for the visuospatial task (A), visuospatial control condition (B), working memory task (C), working memory control condition (D), average contrast (E), cognitive vs. simple motor contrast (F), and 7 T motor task (G). Colour coding represents associated t-values (threshold t = 3; peak t = 6).

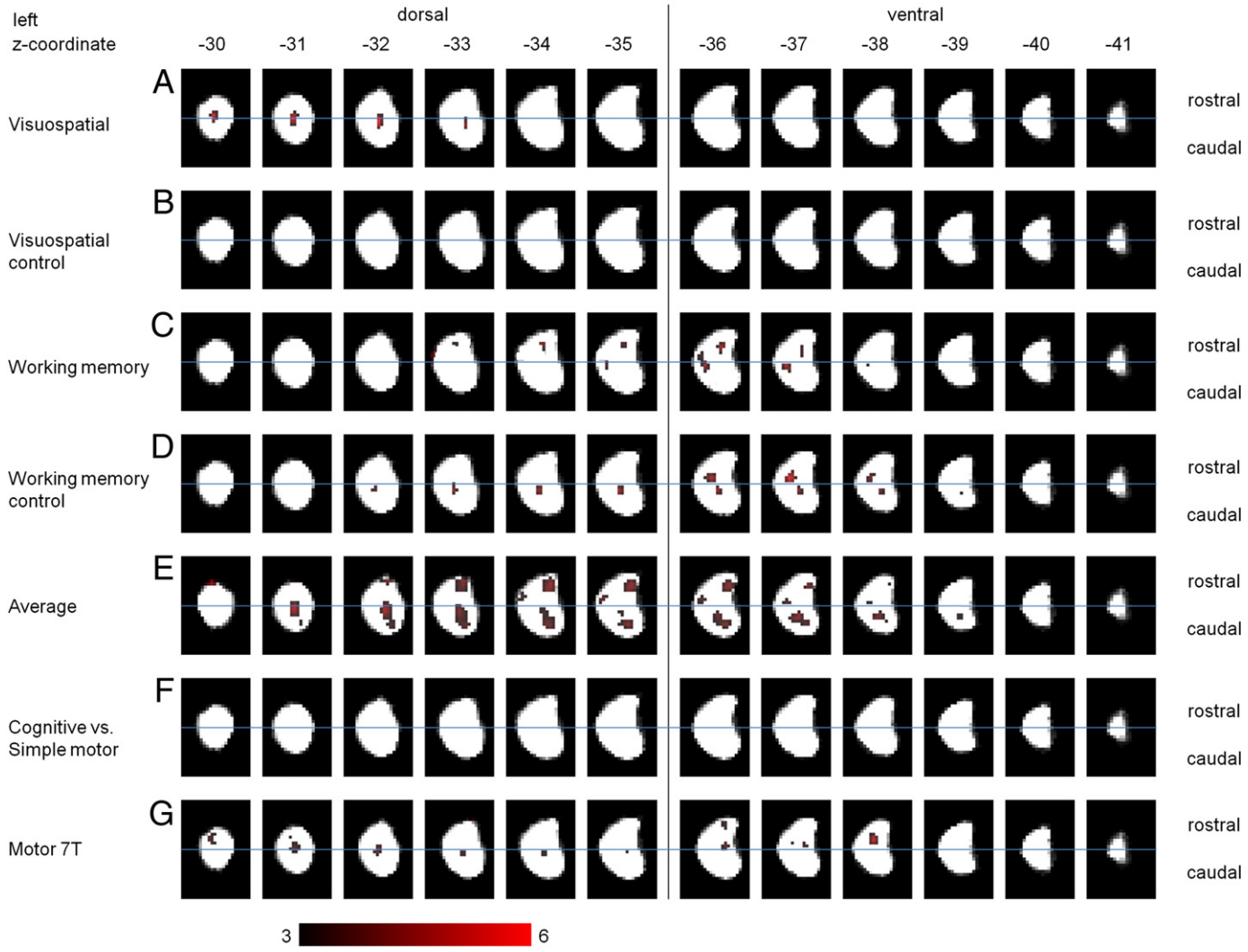

Fig. 7. Significant dentate nucleus activations superimposed on the template of the left nucleus in axial orientation (Diedrichsen et al., 2010) for the visuospatial task (A), visuospatial control condition (B), working memory task (C), working memory control condition (D), average contrast (E), cognitive vs. simple motor contrast (F), and 7 T motor task (G). Colour coding represents associated t-values (threshold t = 3; peak t = 6).

While none of the motor conditions showed reliable activation by themselves, all conditions shared a motor response component. The average contrast therefore should reflect at least partly this component. In this contrast, large clusters were detected with peak activations bilaterally in the dorso-rostral part (Figs. 6E, 7E). On both sides, activations extended to all other parts of the nucleus.

Table 3
Local maxima of dentate nucleus activation ($p<0.005$ unc.) in tasks and conditions showing significant dentate activation. Peak location is underlined.

Contrast	Side	x,y,z	Location	Cluster size	t-value
Visuospatial	Left	−11, −59, −32	DCDN, DRDN	37 mm^3	5.74
	Right	13, −66, −32	DCDN	47 mm^3	5.01
Visuospatial control	Right	20, −64, −36	VCDN, DCDN	88 mm^3	7.19
Working memory	Right	20, −61, −36	VCDN, DCDN	21 mm^3	6.12
	Left	−18, −59, −37	VCDN, VRDN, DCDN	48 mm^3	4.87
	Left	−13, −53, −36	VRDN, DRDN	48 mm^3	4.54
Working memory control	Right	17, −65, −35	DCDN, VCDN	36 mm^3	5.86
	Left	−17, −56, −37	VRDN	26 mm^3	5.41
	Left	−14, −60, −35	VCDN, DCDN	36 mm^3	4.53
Average	Right	12, −52, −33	DRDN, VCDN, VRDN, DCDN	698 mm^3	5.11
	Left	−10, −59, −31	DCDN, VCDN, DRDN	271 mm^3	4.68
	Left	−10, −51, −34	DRDN, VRDN	118 mm^3	4.22
	Left	−19, −56, −36	VRDN, DRDN	50 mm^3	3.67
Cognitive vs. simple motor	Right	13, −68, −33	DCDN, VCDN	53 mm^3	4.6
7 T motor	Right	14, −50. −35	DRDN, VRDN, DCDN	284 mm^3	5.55
	Right	14, −63, −39	VCDN, DCDN	115 mm^3	4.26
	Left	−15, −55, −38	VRDN, DRDN, DCDN	113 mm^3	5.0

DRDN = dorso-rostral dentate nucleus, VCDN = ventro-caudal dentate nucleus, DCDN = dorso-caudal dentate nucleus, VRDN = ventro-rostral dentate nucleus.

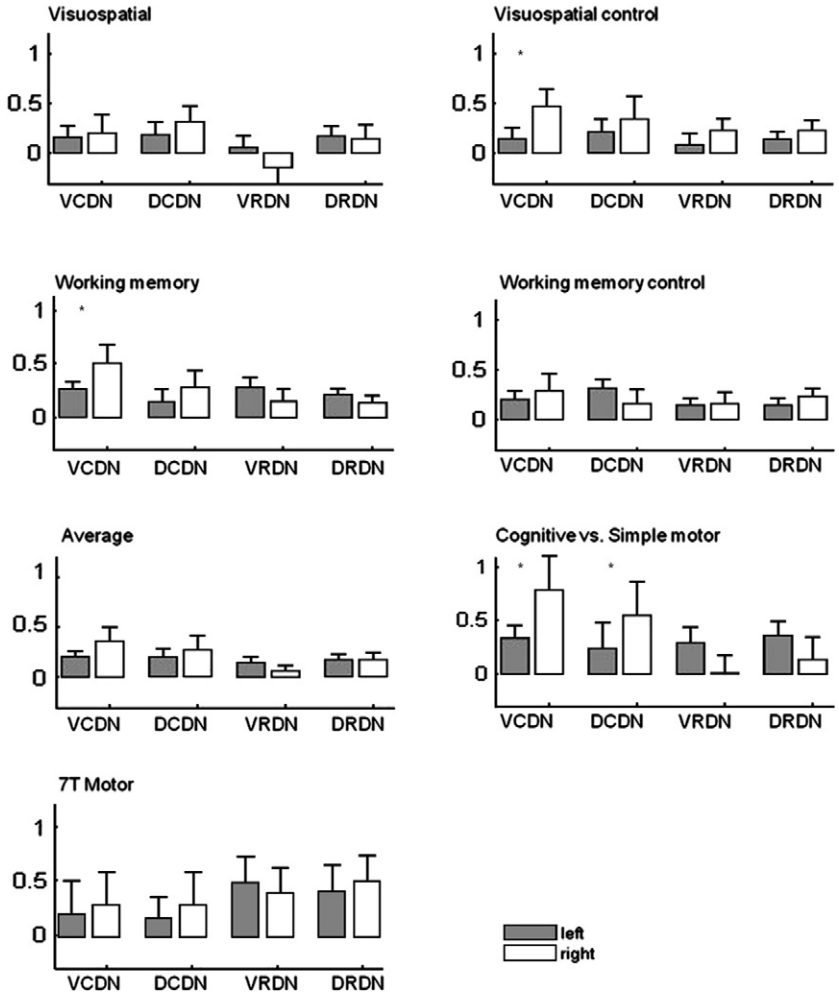

Fig. 8. Effects of lateralization. Means and standard deviations of activation (beta estimates) within each of the four dentate nucleus subdomains on the left and right side are shown for the tasks and conditions with significant activation. Significant side effects are denoted by an * ($p<0.05$, paired t-test). VCDN = ventro-caudal dentate nucleus, DCDN = dorso-caudal dentate nucleus, VRDN = ventro-rostral dentate nucleus, DRDN = dorso-rostral dentate nucleus.

A direct comparison of the cognitive tasks and control conditions did not result in significant activations. To further investigate dentate nucleus non-motor representations, both cognitive tasks were averaged and the simple motor task subtracted from this contrast. This operation led to exclusive caudal dentate activation on the right side.

Effects of lateralization. Statistical analysis revealed significant effects of lateralization within the ventro-caudal dentate nucleus to the right side for the verbal working memory task (Fig. 8). No lateralization effects were observed for the visuospatial task. However, there was right lateralization ventro-caudally in the visuospatial control task. In the contrast "cognitive vs. simple motor", significant right-sided predominance was present within the ventro- and dorso-caudal dentate nucleus.

Experiment 2 (supplementary 7 T MRI data set)

Methods

Participants

A total of 25 healthy male participants (mean age of 28.3 ± 6.4 years) were included. Two participants were excluded because of movement artifacts (head translation > 2 mm). Data from 23 participants (mean age 28.1 ± 6.3 years) were included in group statistical analysis.

fMRI data acquisition

A whole-body 7 T MR scanner (Magnetom 7 T, Siemens Healthcare, Erlangen, Germany) was used to acquire BOLD-contrast-weighted EPIs for functional scans. All fMRI images were acquired with an eight-channel transmit/receive head coil (Rapid Biomedical, Wuerzburg, Germany). Each EPI session consisted of 135 mosaic scans with 45 slices, matrix 128 × 128, TR = 3000 ms, TE = 22 ms, FoV = 256 mm, GRAPPA parallel imaging with acceleration factor 2, TA 6:54 min, flip angle between 49° and 78°, bandwidth 1562 Hz/pixel, sinusoidal readout gradient, slice thickness 1.9 mm, and voxel size = 2.0 × 2.0 × 1.9 mm^3 with 10% distance factor due to ascending mode. The parallel imaging techniques used here have been shown to reduce image distortions and signal loss occurring especially at ultra-highfield fMRI (Poser and Norris, 2009). Because of magnetization relaxation effects, the first five volumes in each session were discarded from further analysis. Scans covered the entire cerebellum in contrast to the 1.5 T data.

Commonly, fMRI studies use a phase-encoding direction anterior ≫ posterior. In this direction the through-plane direction consists amongst others of air-bone and various tissue interfaces in comparison to the homogeneous cerebrum. Due to stronger Nyquist ghosts in the phase-encoding direction at ultra-highfield strengths, artifacts in the cerebellum are common. To avoid these, phase encoding in the feet ≫ head direction was used.

Experimental condition

For the 7 T experiment participants had to perform a simple finger movement motor task. Participants conducted a tapping task with their right index finger while their hand rested on their right thigh. Participants were asked to repeatedly move the index finger two times to the right side (using the maximum lateral movement range of their index finger without wrist movement) and one time to the left side. Participants were asked to perform the movements quickly; however, the participants were allowed to perform the movements at their own pace. An active block was started by a visual presentation of the word "finger", during rest a fixation cross was presented visually. No recordings of the movements were performed.

Image analysis

Image analysis was performed as outlined above (Experiment 1: 1.5 T MRI data set) including participant-wise analysis, which is provided as supplementary material. For the dentate nucleus activations, bootstrap analysis of the 7 T data set based on 23 participants revealed a corrected peak t-value of 4.03 and a minimal cluster size of 27 mm^3 (at $t(23) = 2.82$, $p = 0.005$).

Results

Cerebellar cortical activations

Finger movements were followed by strong activation with a large cluster peaking within the ipsilateral (right) anterior hand area (lobule V), with continuous extension to the left anterior cerebellum and the hand area within the ipsilateral posterior cerebellum (lobule VIII). Neighboring parts of Crus I bilaterally were also activated. On the left side, there were two additional clusters comprising lobules VII and VIII in the posterior cerebellum (Table 2, Fig. 5).

Dentate nucleus activations

Strongest activation was detected in the ipsilateral (right) dorso-rostral dentate (Table 3, Figs. 6G and 7G). This cluster also involved parts of the ventro-rostral and dorso-caudal dentate. One other smaller ipsilateral cluster was found in the ventro-caudal dentate. On the contralateral (left) side, there was one cluster peaking ventro-rostrally extending to the dorso-rostral and dorso-caudal dentate.

Discussion

Strongest activations in the dentate nucleus were seen in the cognitive tasks. Both verbal working memory and visuospatial demands lead to activations which are most significant in the caudal parts of the dentate. Significant effects of lateralization were found for the verbal working memory but not the visuospatial task. After subtraction of the simple motor task from cognitive average contrast, exclusive caudal activation remained. Motor-related activation was lower with no significant activation in the two motor tasks. However, a common analysis of all conditions revealed extended activation of the dorso-rostral dentate nucleus. Because all tasks required movement of the fingers or wrist of the right hand, dorso-rostral activation is most likely explained by motor activation. These results are supported by a supplementary motor experiment using 7 T MRI, which revealed strong dorso-rostral activations. The findings are consistent with a subdivision of the dentate nucleus into a motor and non-motor domain in humans, which has been proposed by Dum and Strick (2003) based on anatomical findings in monkeys.

Cerebellar cortical activations

1.5 T MRI scanning focused on the DCN and did not include all parts of the cerebellar cortex. The cerebellar cortical areas known to be related to hand movements, verbal working memory, and visuospatial tasks were included only in part based on previous brain imaging studies (Stoodley and Schmahmann, 2009).

All 1.5 T MRI tasks included right-sided movements. As expected, all tasks were followed by activations of the well-known hand areas in lobules VI and VIII (Rijntjes et al., 1999; Grodd et al., 2001; Stoodley and Schmahmann, 2009). Parts of the superior hand area, that is most of lobule V (as well as the rest of the anterior lobe), however, were not included in the field of view. This explains why activation of the superior hand area was seen in the complex but not the simple movement task. Activation was most prominent on the side ipsilateral to the movement. In the complex motor and the working memory tasks less prominent contralateral activation was also present. Contralateral activation is in good agreement with the previous brain imaging literature. Significant contralateral activation was missing in the visuospatial tasks, possibly because the number of required movements was significantly less compared to the motor and working memory tasks (visuospatial task: 20 movements per block; motor task: 90 movements per block; memory task: 40 movements per block). Vermal activation was more prominent in the verbal working memory and visuospatial tasks compared to the motor tasks. The motor task was performed with eyes closed. Vermal activation in the cognitive tasks is likely related to accompanying eye movements.

A recent meta-analysis by Stoodley and Schmahmann (2009) showed that verbal working memory tasks are followed by activation within cerebellar cortical lobules VI, Crus I (bilateral), and VIII A (right-sided), whereas visuospatial tasks activate primarily VI (left predominant). Accordingly, in the present verbal working memory task activation of Crus I was stronger compared to the visuospatial task. The right inferior cerebellum has also been linked to verbal working memory (Chen and Desmond, 2005; Stoodley and Schmahmann, 2009). The known peak location within lobule VIII A ($z = -60$, see Table 3 in meta-analysis by Stoodley and Schmahmann, 2009), however, was outside our field of view. Likewise, cerebellar cortical regions associated with visuospatial abilities were also not imaged in our study (peaks at $z = -18$ and -22 in left lobule VI as reported by Stoodley and Schmahmann, 2009).

The supplementary 7 T MRI motor experiment included all parts of the cerebellum and showed activations of the known hand areas within the anterior and posterior cerebellum including lobule IV and V, which were not imaged in the 1.5 T data set. Activations were accentuated on the ipsilateral side.

Dentate nucleus activations

In the cognitive tasks, most significant activation was observed in the caudal parts of the nucleus. In the verbal working memory task, right-sided activation of the ventro-caudal dentate predominated. Some ventro-caudal activation was present on the left as well; however, statistical analysis revealed significant predominance of the right side within the ventro-caudal part (Fig. 8). Peak activations within the ventro-caudal dentate correspond well to Dum and Strick's unfolded map (Dum and Strick, 2003; Strick et al., 2009). The ventro-caudal dentate was shown to be connected to BA 46d and BA 9 L in the dorsolateral prefrontal cortex (Middleton and Strick, 1994, 2001; Dum and Strick, 2003). Both areas take part in human verbal working memory (Smith and Jonides, 1998; Ray et al., 2008). Furthermore, Desmond et al. (1997) found a lateralization of verbal working memory function to the right cerebellar cortex, which is in accordance with our results showing ventro-caudal dentate activations predominantly on the right (see also meta-analysis of Stoodley and Schmahmann, 2009). A recent fMRI study (Hautzel et al., 2009), however, did not find any lateralization effects in the cerebellar cortex during working memory tasks. Lateralization to the right may be due to the verbal component of the task, and not the working memory requirement per se. Language tasks have been shown to lateralize to the right cerebellar hemisphere (Frings et al., 2006). The activation pattern seen in the working memory

control task was very similar to that observed in the working memory task except pronounced ventro-caudal activation with lateralization to the right in the working memory task. Both tasks showed bilateral dorso-caudal activations, which may be a consequence of some visuospatial demand (that is movement to the four buttons of the touchpad in space according to visual input) in these tasks.

In fact, most significant activations in the visuospatial task were detected in the dorso-caudal dentate. Dum and Strick (2003) showed that connections to BA 7b in the inferior parietal lobule originate within the ventral portion of the caudal dentate with some extension into the dorso-caudal dentate, while projections to the AIP originate mainly from the dorso-caudal dentate (Clower et al., 2005; Fig. 1). BA 7b and AIP are thought to be involved in the visual guidance of movements (Andersen, 1989; Colby and Goldberg, 1999; Clower et al., 2005). Therefore, dorso-caudal activation is consistent with anatomical observations in the monkey, although one might have expected additional activation of ventro-caudal parts. The visuospatial control task further substantiates that caudal activation is due to the visuospatial requirements. In the control task, movement requirements were the same, but visuospatial requirements were significantly reduced. In the visuospatial control task, no cluster peaking in the dorso-caudal dentate activation was present. Instead, there was a strong ipsilateral ventro-caudal activation present. Because participants had to perform a certain motor sequence repeatedly within one active block, motor learning may have driven ventro-caudal activation. Ipsilateral dentate nucleus activation together with activation of Crus I and lobule VI, which was found also in the visuospatial control task, has been reported as a typical activation pattern during motor sequence learning (Doyon et al., 2002; Penhune and Doyon, 2005).

Different to our expectations, there was no significant lateralization to the left, although activation of the left caudal dentate was present only in the visuospatial task but not the visuospatial control task. In contrast to language tasks, however, previous findings in behavioural and imaging studies regarding lateralization of visuospatial function are mixed. Whereas predominant activation of the left cerebellar cortex was reported in previous fMRI studies investigating line bisection tasks and in one meta-analysis (Fink et al., 2000, 2001; Stoodley and Schmahmann, 2009), other neuroimaging studies investigating mental navigation and mental rotation found exclusive right (Jordan et al., 2001; Ino et al., 2002) or bilateral cerebellar activations (Parsons et al., 1995). Likewise, there are human cerebellar lesion studies reporting left-sided lateralization (Baillieux et al., 2009), whereas others showed no clear lateralization (Molinari et al., 2004).

Compared to the cognitive tasks, dentate activation was much lower and below the selected level of significance in the two motor tasks imaged at 1.5 T. As motor function of the right hand was necessary in every condition, we created an average contrast including all tasks to maximize statistical power. The contrast showed strong dorso-rostral activation. Because this activation was not present in any of the individual tasks and all tasks required comparable movements, dorso-rostral activation likely represents movement-related activity. To further support the site of motor activation within the dentate nucleus, we acquired an additional data set at 7 T using the advantages of superior signal-to-noise ratio (SNR) and increased (factor 2–3) BOLD contrast compared to 1.5 T imaging (Gizewski et al., 2007). This data set revealed strong bilateral dorso-rostral dentate activation (accentuated on the ipsilateral side), paralleling the 1.5 T average contrast. Our findings fit to the assumption put forward by Dum and Strick that the more dorso-rostral parts of the dentate are related to motor function (see Fig. 1). Similar to motor-related activations of the cerebellar cortex, dorso-rostral activations were not restricted to the ipsilateral side. The 7 T motor task also produced some caudal activation on the ipsilateral side. The cluster was considerably smaller than the rostral cluster and may have been driven by the minor cognitive demands of the task. Cognitive demands were reduced compared to the 1.5 T tasks (e.g. no auditory pacing was necessary). However, just as the cognitive tasks included some motor requirements (e.g. inner speech in the verbal memory task, pressing of response keys), cognitive requirements in the voluntary movement tasks could not be fully excluded (e.g. to remember and follow the instructed motor sequence).

The findings appear to be at variance with earlier findings of our group. Our previous 1.5 T study found ipsilateral caudal dentate nucleus activation in a finger tapping task which was comparable to the complex motor condition in the present 1.5 T study (Dimitrova et al., 2006a). Peak maxima in this study were found in the cerebellar cortex and extended continuously into the cerebellar nuclei region (see Fig. 5 in Dimitrova et al., 2006a). However, in that study normalization was performed using standard SPM methods which suffer from poor overlap between participants within the dentate in group statistical analysis. Furthermore, there is a substantial danger that reported activations of the dentate may be due to activation from surrounding gray matter structures smoothed into the nucleus (Type II error), especially given that a smoothing kernel of 6 mm FWHM was used. In fact, a new analysis of these data applying the improved normalization protocol used in the current study did not lead to any statistically significant activation within the DCN. Likewise, reanalysis of the present data set with the same standard SPM normalization revealed caudal dentate activation in the motor tasks (supplementary materials).

We did not find any reliable differences between the cognitive tasks and control conditions. This was also true for the cerebellar cortex. In hindsight, the control conditions contained many of the task demands of the real tasks. For example, in the working memory control condition, participants needed to translate the digits to movements in each trial. Behavioural data available for the working memory task and its control condition further supports the assumption that the cognitive demands in these tasks were comparable, as there was no significant difference in the average error rate (Table 1). Indeed, the visuospatial control condition may have engaged cortico-cerebellar circuits more due to learning. Therefore, we created the "cognitive vs. simple motor" contrast to detect non-motor domains within the dentate nucleus. This contrast showed ipsilateral activation in the ventro- and dorso-caudal compartment. As outlined above, the ventro-caudal dentate has been shown to project to prefrontal areas, whereas both the dorso-caudal as well as the ventro-caudal dentate project to parietal areas. This result is consistent with the representation of non-motor areas proposed by Dum and Strick which are thought to support working memory and visuospatial function. Missing contralateral activation is likely a consequence of right-sided lateralization of working memory function.

Overall dentate activation was mainly driven by cognitive requirements represented in the caudal dentate. These findings parallel results showing that dentate activation in fMRI increases in tasks which require planning/executive function (Kim et al., 1994) or sensory information processing (Gao et al., 1996; Parsons et al., 1997; Liu et al., 2000) compared to simple motor tasks (for recent review see: Habas, 2010).

Limitations

A major limitation of the present study is that the cognitive and control tasks did not differ enough in order to reveal dentate nucleus non-motor domains by means of direct task subtractions. We therefore used the "cognitive vs. simple motor" contrast to show dentate nucleus regions related to non-motor function. Therefore, these findings need to be confirmed using improved motor and non-motor paradigms. Of further note, eye movements were not recorded. Thus, it cannot be excluded that part of the findings are explained by different demands on eye movements and visual control of movements (Glickstein et al., 2009). Additional improvement of the data sets could have been reached by using recent methods to control for physiological artifacts caused by breathing and vessel pulsation (for a review, see: Diedrichsen et al., 2010) as well as the use of EPI field maps to compensate for field inhomogeneities (Hutton et al., 2002).

Conclusions

Our results are consistent with a subdivision of the dentate nucleus into a motor and non-motor domain in humans as proposed in monkeys (Dum and Strick, 2003). Overall, cognitive task performance appears to be followed by stronger dentate activation than simpler motor tasks. Motor-related areas can be found in the dorso-rostral dentate. Caudal parts of the dentate support cognitive function.

Supplementary materials related to this article can be found online at doi:10.1016/j.neuroimage.2010.11.028.

Acknowledgments

This work was supported by DFG TI 239/9-1.

References

Allen, G., McColl, R., Barnard, H., Ringe, W.K., Fleckenstein, J., Cullum, C.M., 2005. Magnetic resonance imaging of cerebellar–prefrontal and cerebellar–parietal functional connectivity. Neuroimage 28, 39–48.

Andersen, R.A., 1989. Visual and eye movement functions of the posterior parietal cortex. Annu. Rev. Neurosci. 12, 377–403.

Baillieux, H., De Smet, H.J., Dobbeleir, A., Paquier, P.F., De Deyn, P.P., Mariën, P., 2009. Cognitive and affective disturbances following focal cerebellar damage in adults: a neuropsychological and SPECT study. Cortex. Available at http://www.ncbi.nlm.nih.gov/pubmed/19853848.

Chen, S.H.A., Desmond, J.E., 2005. Temporal dynamics of cerebro-cerebellar network recruitment during a cognitive task. Neuropsychologia 43, 1227–1237.

Clower, D.M., Dum, R.P., Strick, P.L., 2005. Basal ganglia and cerebellar inputs to 'AIP'. Cereb. Cortex 15, 913–920.

Colby, C.L., Goldberg, M.E., 1999. Space and attention in parietal cortex. Annu. Rev. Neurosci. 22, 319–349.

Desmond, J.E., Gabrieli, J.D., Wagner, A.D., Ginier, B.L., Glover, G.H., 1997. Lobular patterns of cerebellar activation in verbal working-memory and finger-tapping tasks as revealed by functional MRI. J. Neurosci. 17, 9675–9685.

Diedrichsen, J., 2006. A spatially unbiased atlas template of the human cerebellum. Neuroimage 33, 127–138.

Diedrichsen, J., Maderwald, S., Küper, M., Thürling, M., Rabe, K., Gizewski, E.R., Ladd, M.E., Timmann, D., 2010. Imaging the deep cerebellar nuclei: a probabilistic atlas and normalization procedure. Neuroimage. Available at http://www.ncbi.nlm.nih.gov/pubmed/20965257.

Diedrichsen, J., Balsters, J.H., Flavell, J., Cussans, E., Ramnani, N., 2009. A probabilistic MR atlas of the human cerebellum. Neuroimage 46, 39–46.

Diedrichsen, J., Verstynen, T., Schlerf, J., Wiestler, T., 2010. Advances in functional imaging of the human cerebellum. Curr. Opin. Neurol. 23, 382–387.

Dimitrova, A., de Greiff, A., Schoch, B., Gerwig, M., Frings, M., Gizewski, E.R., Timmann, D., 2006a. Activation of cerebellar nuclei comparing finger, foot and tongue movements as revealed by fMRI. Brain Res. Bull. 71, 233–241.

Dimitrova, A., Zeljko, D., Schwarze, F., Maschke, M., Gerwig, M., Frings, M., Beck, A., Aurich, V., Forsting, M., Timmann, D., 2006b. Probabilistic 3D MRI atlas of the human cerebellar dentate/interposed nuclei. Neuroimage 30, 12–25.

Doyon, J., Song, A.W., Karni, A., Lalonde, F., Adams, M.M., Ungerleider, L.G., 2002. Experience-dependent changes in cerebellar contributions to motor sequence learning. Proc. Natl. Acad. Sci. U. S. A. 99, 1017–1022.

Dum, R.P., Strick, P.L., 2003. An unfolded map of the cerebellar dentate nucleus and its projections to the cerebral cortex. J. Neurophysiol. 89, 634–639.

Fink, G.R., Marshall, J.C., Shah, N.J., Weiss, P.H., Halligan, P.W., Grosse-Ruyken, M., Ziemons, K., Zilles, K., Freund, H.J., 2000. Line bisection judgments implicate right parietal cortex and cerebellum as assessed by fMRI. Neurology 54, 1324–1331.

Fink, G.R., Marshall, J.C., Weiss, P.H., Zilles, K., 2001. The neural basis of vertical and horizontal line bisection judgments: an fMRI study of normal volunteers. Neuroimage 14, S59–S67.

Frings, M., Dimitrova, A., Schorn, C.F., Elles, H., Hein-Kropp, C., Gizewski, E.R., Diener, H.C., Timmann, D., 2006. Cerebellar involvement in verb generation: an fMRI study. Neurosci. Lett. 409, 19–23.

Friston, K.J., Frith, C.D., Turner, R., Frackowiak, R.S., 1995. Characterizing evoked hemodynamics with fMRI. Neuroimage 2, 157–165.

Gao, J.H., Parsons, L.M., Bower, J.M., Xiong, J., Li, J., Fox, P.T., 1996. Cerebellum implicated in sensory acquisition and discrimination rather than motor control. Science 272, 545–547.

Gizewski, E.R., de Greiff, A., Maderwald, S., Timmann, D., Forsting, M., Ladd, M.E., 2007. fMRI at 7 T: whole-brain coverage and signal advantages even infratentorially? Neuroimage 37, 761–768.

Gizewski, E.R., Maderwald, S., Wanke, I., Goehde, S., Forsting, M., Ladd, M.E., 2005. Comparison of volume, four- and eight-channel head coils using standard and parallel imaging. Eur. Radiol. 15, 1555–1562.

Glickstein, M., Sultan, F., Voogd, J., 2009. Functional localization in the cerebellum. Cortex. Available at http://www.ncbi.nlm.nih.gov/pubmed/19833328.

Grodd, W., Hülsmann, E., Lotze, M., Wildgruber, D., Erb, M., 2001. Sensorimotor mapping of the human cerebellum: fMRI evidence of somatotopic organization. Hum. Brain Mapp. 13, 55–73.

Gurd, J.M., Amunts, K., Weiss, P.H., Zafiris, O., Zilles, K., Marshall, J.C., Fink, G.R., 2002. Posterior parietal cortex is implicated in continuous switching between verbal fluency tasks: an fMRI study with clinical implications. Brain 125, 1024–1038.

Habas, C., 2010. Functional imaging of the deep cerebellar nuclei: a review. Cerebellum 9, 22–28.

Habas, C., Kamdar, N., Nguyen, D., Prater, K., Beckmann, C.F., Menon, V., Greicius, M.D., 2009. Distinct cerebellar contributions to intrinsic connectivity networks. J. Neurosci. 29, 8586–8594.

Hautzel, H., Mottaghy, F.M., Specht, K., Müller, H., Krause, B.J., 2009. Evidence of a modality-dependent role of the cerebellum in working memory? An fMRI study comparing verbal and abstract n-back tasks. Neuroimage 47, 2073–2082.

Hayasaka, S., Nichols, T.E., 2003. Validating cluster size inference: random field and permutation methods. Neuroimage 20, 2343–2356.

Hutton, C., Bork, A., Josephs, O., Deichmann, R., Ashburner, J., Turner, R., 2002. Image distortion correction in fMRI: a quantitative evaluation. Neuroimage 16, 217–240.

Ino, T., Inoue, Y., Kage, M., Hirose, S., Kimura, T., Fukuyama, H., 2002. Mental navigation in humans is processed in the anterior bank of the parieto-occipital sulcus. Neurosci. Lett. 322, 182–186.

Jordan, K., Heinze, H.J., Lutz, K., Kanowski, M., Jäncke, L., 2001. Cortical activations during the mental rotation of different visual objects. Neuroimage 13, 143–152.

Jueptner, M., Frith, C.D., Brooks, D.J., Frackowiak, R.S., Passingham, R.E., 1997. Anatomy of motor learning. II. Subcortical structures and learning by trial and error. J. Neurophysiol. 77, 1325–1337.

Kim, S.G., Uğurbil, K., Strick, P.L., 1994. Activation of a cerebellar output nucleus during cognitive processing. Science 265, 949–951.

Lee, T.M.C., Liu, H., Hung, K.N., Pu, J., Ng, Y., Mak, A.K.Y., Gao, J., Chan, C.C.H., 2005. The cerebellum's involvement in the judgment of spatial orientation: a functional magnetic resonance imaging study. Neuropsychologia 43, 1870–1877.

Liu, Y., Pu, Y., Gao, J.H., Parsons, L.M., Xiong, J., Liotti, M., Bower, J.M., Fo, P.T., 2000. The human red nucleus and lateral cerebellum in supporting roles for sensory information processing. Hum. Brain Mapp. 10, 147–159.

Malm, J., Kristensen, B., Karlsson, T., Carlberg, B., Fagerlund, M., Olsson, T., 1998. Cognitive impairment in young adults with infratentorial infarcts. Neurology 51, 433–440.

Miall, R.C., Reckess, G.Z., Imamizu, H., 2001. The cerebellum coordinates eye and hand tracking movements. Nat. Neurosci. 4, 638–644.

Middleton, F.A., Strick, P.L., 1994. Anatomical evidence for cerebellar and basal ganglia involvement in higher cognitive function. Science 266, 458–461.

Middleton, F.A., Strick, P.L., 2001. Cerebellar projections to the prefrontal cortex of the primate. J. Neurosci. 21, 700–712.

Molinari, M., Petrosini, L., Misciagna, S., Leggio, M., 2004. Visuospatial abilities in cerebellar disorders. J. Neurol. Neurosurg. Psychiatry 75, 235–240.

Molinari, M., Leggio, M.G., 2007. Cerebellar information processing and visuospatial functions. Cerebellum 6, 214–220.

Oldfield, R.C., 1971. The assessment and analysis of handedness: the Edinburgh inventory. Neuropsychologia 9, 97–113.

Parsons, L.M., Bower, J.M., Gao, J.H., Xiong, J., Li, J., Fox, P.T., 1997. Lateral cerebellar hemispheres actively support sensory acquisition and discrimination rather than motor control. Learn. Mem. 4, 49–62.

Parsons, L.M., Fox, P.T., Downs, J.H., Glass, T., Hirsch, T.B., Martin, C.C., Jerabek, P.A., Lancaster, J.L., 1995. Use of implicit motor imagery for visual shape discrimination as revealed by PET. Nature 375, 54–58.

Penhune, V.B., Doyon, J., 2005. Cerebellum and M1 interaction during early learning of timed motor sequences. Neuroimage 26, 801–812.

Pimenta, A.F., Strick, P.L., Levitt, P., 2001. Novel proteoglycan epitope expressed in functionally discrete patterns in primate cortical and subcortical regions. J. Comp. Neurol. 430, 369–388.

Poser, B.A., Norris, D.G., 2009. Investigating the benefits of multi-echo EPI for fMRI at 7 T. Neuroimage 45, 1162–1172.

Ravizza, S.M., McCormick, C.A., Schlerf, J.E., Justus, T., Ivry, R.B., Fiez, J.A., 2006. Cerebellar damage produces selective deficits in verbal working memory. Brain 129, 306–320.

Ray, M.K., Mackay, C.E., Harmer, C.J., Crow, T.J., 2008. Bilateral generic working memory circuit requires left-lateralized addition for verbal processing. Cereb. Cortex 18, 1421–1428.

Rijntjes, M., Buechel, C., Kiebel, S., Weiller, C., 1999. Multiple somatotopic representations in the human cerebellum. NeuroReport 10, 3653–3658.

Schmahmann, J.D., 2004. Disorders of the cerebellum: ataxia, dysmetria of thought, and the cerebellar cognitive affective syndrome. J. Neuropsychiatry Clin. Neurosci. 16, 367–378.

Silveri, M.C., Di Betta, A.M., Filippini, V., Leggio, M.G., Molinari, M., 1998. Verbal short-term store-rehearsal system and the cerebellum. Evidence from a patient with a right cerebellar lesion. Brain 121 (Pt 11), 2175–2187.

Smith, E.E., Jonides, J., 1998. Neuroimaging analyses of human working memory. Proc. Natl. Acad. Sci. U. S. A. 95, 12061–12068.

Stanton, G.B., 1980. Topographical organization of ascending cerebellar projections from the dentate and interposed nuclei in *Macaca mulatta*: an anterograde degeneration study. J. Comp. Neurol. 190, 699–731.

Stoodley, C.J., Schmahmann, J.D., 2010. Evidence for topographic organization in the cerebellum of motor control versus cognitive and affective processing. Cortex. Available at http://www.ncbi.nlm.nih.gov/pubmed/20152963.

Stoodley, C.J., Schmahmann, J.D., 2009. Functional topography in the human cerebellum: a meta-analysis of neuroimaging studies. Neuroimage 44, 489–501.

Strick, P.L., Dum, R.P., Fiez, J.A., 2009. Cerebellum and nonmotor function. Annu. Rev. Neurosci. 32, 413–434.

Thach, W.T., Perry, J.G., Kane, S.A., Goodkin, H.P., 1993. Cerebellar nuclei: rapid alternating movement, motor somatotopy, and a mechanism for the control of muscle synergy. Rev. Neurol. (Paris) 149, 607–628.